Versatile chiroptics of peptide-induced assemblies of metalloporphyrins†

Hirokuni Jintoku,[a] Takashi Sagawa,[b] Tsuyoshi Sawada,[a] Makoto Takafuji[a] and Hirotaka Ihara*[a]

Received 25th September 2009, Accepted 30th November 2009
First published as an Advance Article on the web 14th January 2010
DOI: 10.1039/b920058d

Zinc porphyrin functionalized with double long-chain alkylated L-glutamide (**GTPP-Zn**) was synthesized for the first time, and its self-assembling behaviour was investigated in nonpolar organic solvents. The uniqueness of this functionalized porphyrin is characterized by its drastic colour change from dark green to purple *via* the formation of chirally stacked structures through selective axial coordination on zinc with pyridine derivatives. In this paper, we report the versatility of the **GTPP-Zn** assembly process as a stimuli-responsive chiroptical switching system and describe the remarkable ligand-specific induction of secondary chirality accompanied by aggregation morphological change.

Introduction

Chiroptics is important for the investigation of chiral substances in nature. These optical techniques can be used to create complicated nanostructures from chiral molecules such as amino acids and sugars. Recently, chiroptical materials have come to be used in diverse fields such as analytical chemistry, photochemistry, and materials chemistry.[1] Thus, nanofabrication with chiroptical molecules holds significant promise as a method to realize molecular devices with possible applications such as chiroptical switches, films, and molecular motors.[2]

Furthermore, molecular organogel systems have been widely investigated as unique organic media in which gelation occurs through the formation of a three-dimensional nanofibrillar network of self-assembling low-molecular-weight compounds such as peptide-, sugar- and cholesterol-based lipophilic compounds.[3] The fibrillar aggregates are often chirally ordered and show secondary chirality with strong CD signals in organic media. Successfully synthesized examples include pyrene-, perylene-, isoquinoline-, triazine- and porphyrin-containing organogel systems.[4] Therefore, a molecular organogel system is an attractive candidate for chiroptical materials.

On the basis of these viewpoints, we focus on chiroptical porphyrin derivatives with the aim of creating stimuli-responsive soft materials. Herein, we introduce a novel chiroptical molecule (**GTPP-Zn**) containing a zinc porphyrin unit that is functionalized with a double long-chain alkylated L-glutamide derivative as a promoter for chiral assembly (Scheme 1). It is expected that chiral stacking of porphyrin units can not only be induced through intermolecular hydrogen bonding between the L-glutamide units[5] but also be tuned by axial coordination on zinc.[6]

In this paper, we report the versatility of the **GTPP-Zn** self-assembling system as a stimuli-responsive chiroptical switch, exhibiting a remarkable ligand-specific spectral shift, induction of secondary chirality, and dynamic morphological change.

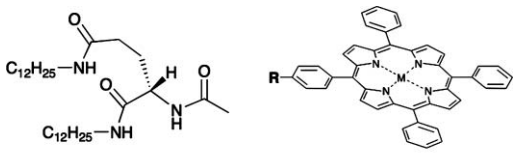

M = 2H, R = H : **TPP**
M = 2H, R = G : **GTPP**
M = Zn, R = H : **TPP-Zn**
M = Zn, R = G : **GTPP-Zn**

Scheme 1 L-Glutamide-derivatives functionalized tetraphenylporphyrin.

Results and discussion

Solubility change of the porphyrin derivative by zinc-insertion

The free-base tetraphenylporphyrin (**TPP**) derivative functionalized with L-glutamide-derived lipid (**GTPP**) showed almost no solubility in nonpolar organic solvents such as diethyl ether, cyclohexane and n-hexane. However, we observed that this limited solubility promotes gelation in organic media through nanofibrillar aggregation when solvent polarity is adjusted with polar solvents such as THF and DMF.[7] This phenomenon is a form of low-molecular-mass organogelation.[8]

Interestingly, zinc insertion into **GTPP** resulted in remarkably improved solubility in nonpolar organic solvents while the gelation ability almost disappeared.† Good solubility is a significant advantage in the manufacture of soft materials. Reduction of the solvent absorption, especially in the UV region, is also important. As shown in Fig. 1a, a deep pink-coloured clear solution (0.25 mM) was obtained without any gelation at 20 °C when zinc-containing **GTPP** (**GTPP-Zn**) was dissolved in cyclohexane. The λ_{max} of the glutamide-unit-free **TPP** moiety was located at 430 nm as a single peak, which was longer by 13 nm than that in zinc-containing **TPP** (Fig. 1a). This indicates aggregation of **GTPP-Zn** in cyclohexane. To address this observation, the following were examined: (1) λ_{max} of **GTPP-Zn** shifted from 430 nm to 417 nm by high dilution such as to 1 μM. The spectral pattern with λ_{max} of 417 nm is

[a]*Department of Applied Chemistry & Biochemistry, Kumamoto University, 2-39-1 Kurokami, Kumamoto, 860-8555, Japan. E-mail: ihara@kumamoto-u.ac.jp; Fax: (+81) 96 3423662; Tel: (+81) 96 3423661*
[b]*Institute of Advanced Energy, Kyoto University, Gokasho, Uji, Kyoto, 611-0011, Japan. E-mail: t-sagawa@iae.kyoto-u.ac.jp; Fax: (+81) 774 383508; Tel: (+81) 774 384580*

† Electronic supplementary information (ESI) available: Solubility and UV-visible, circular dichroism (CD), ^{1}H-NMR and FT-IR spectra of **GTPP-Zn**. See DOI: 10.1039/b920058d

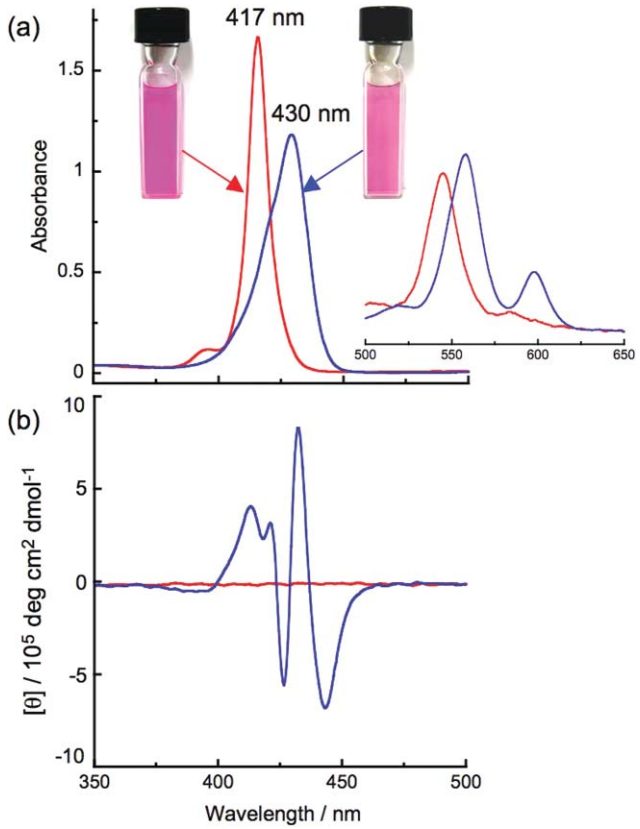

Fig. 1 UV-visible (a) and CD spectra (b) of **TPP-Zn** (red line) and **GTPP-Zn** (blue line) in cyclohexane (0.25 mM) at 20 °C.

similar to that in the Soret band of **TPP-Zn**.† (2) At 10 μM, a reversible λ_{max} shift between 430 nm and 417 nm was observed in the temperature range between 10 °C and 60 °C.† (3) The CD spectra of **GTPP-Zn** showed large Cotton effects ($[\theta]_{433} = 8 \times 10^5$ deg cm^2 dmol^{-1} at 0.25 mM at 20 °C) around the Soret band (Fig. 1b), indicating chiral ordering of a porphyrin moiety while almost no CD was observed at 10 μM at 60 °C or in a highly diluted solution such as 1 μM at 10 °C. These results indicate that **GTPP-Zn** in cyclohexane can disperse as certain aggregates through the amide bonds and also undergoes both lyotropic and thermotropic aggregate–monomer phase transitions.

Chiroptical response to pyridine doping on GTPP-Zn

Addition of pyridine as a ligand to **GTPP-Zn** induced an amazing colour change from deep pink to dark green while **TPP-Zn** showed only a slight change from deep pink to purple, and almost no colour change was observed in free-base **GTPP**. The typical results of the colour changes are summarized in Fig. 2. Hu *et al.* reported that tetra(4-pyridyl)porphyrin formed greenish nanoprisms (rod-like nanocrystals) with assistance from cetyltrimethylammonium bromide as a cationic micellar compound,[9] but there are few similar findings in reports of other synthetic porphyrin systems.[10] Therefore, these observations suggest that pyridine promotes a change in aggregation morphology of **GTPP-Zn** into strongly stacked structures such as nanocrystals. A detailed discussion appears in the next section.

The colour change of **GTPP-Zn** with 10 equiv. of pyridine was accompanied by complicated splitting of the Soret band in the UV-visible spectrum. As shown in Fig. 3a, four peak maxima are observed at 400, 427, 435 and 459 nm. Here, we initially focus on the peak maximum at 427 nm because **TPP-Zn** shows a simple λ_{max} shift from 417 nm to 427 nm by addition of an equimolar amount of pyridine (Fig. 2g). This can be explained by formation of a typical one-to-one complex *via* a nitrogen–zinc coordination.[11] A similar λ_{max} of 427 nm was also observed in **GTPP-Zn** in the presence of a large excess (2000 equimolar) of pyridine (Fig. 2c and 3a). This indicates that pyridine can be an effective solvent for **GTPP-Zn** as well as a ligand for coordination. In support of this, when pyridine-d_5 was used as a solvent in NMR spectroscopy, no peak-broadening phenomenon was observed, indicating complete disaggregation of an L-glutamide derivative. This is probably due to inhibition by pyridine of intermolecular interaction such as hydrogen bonding. Therefore, we conclude that a peak maximum at 427 nm can be attributed to axial coordination of pyridine on **GTPP-Zn** without any aggregation.

The detailed concentration dependency of pyridine is shown in Fig. 4. Neither significant colour nor spectral changes were observed in the presence of 0–4 equiv. of pyridine. It seems that the colour change to dark green (Fig. 2b) is specifically induced in the presence of 5–100 equiv. of pyridine with an increase in the absorbance at 459 nm (Abs_{459}). Further addition of pyridine changes the colour to purple (Fig. 2c) with a decrease in Abs_{459}. However, we found that a greenish colour was observed even in a one-to-one mixture of **GTPP-Zn** and an equimolar amount of pyridine. This was obtained by the following special procedure: when the one-to-one mixture was aged at 60 °C for 10 min and then allowed to stand at 25 °C for two days. Therefore, it is estimated that a one-to-one complex can be produced but is delayed due to the aggregation.

Aggregation structure of the greenish complex

The greenish complex with λ_{max} of 459 nm should be furthermore discussed in detail because it is expected to be a model system for a natural chlorophyll system.[10] As shown in Fig. 3b, the complexation with pyridine was accompanied by an extreme enhancement of CD intensity at around 459 nm. The largest value can be detected in the concentration range of 5–100 equiv. of pyridine and exceeds 1×10^7 deg cm^2 dmol^{-1} in $[\theta]_{462}$ (Fig. 3b), which was 20 times larger than that of the original **GTPP-Zn** aggregates. On the other hand, a decrease of CD intensity was observed in free-base **GTPP** (15 to 0.08×10^4 deg cm^2 dmol^{-1}). Therefore, it is considered that the axial coordination of pyridine on **GTPP-Zn** promotes a drastic change of chirally ordered structures as well as strong stacking among the porphyrin moieties.

On the other hand, the Q band absorptions are also help to understand the molecular aggregation of **GTPP-Zn**. It is known that an absorption spectrum of normal metalloporphyrin shows the other two absorption maxima called the Q or α and β bands, which are found between 500 and 650 nm.[11] As shown in Fig. 3a, the complexation with pyridine induced a relative intensity change of the α and β bands ($\varepsilon_\alpha/\varepsilon_\beta$) as well as a λ_{max} shift. Generally, the value of $\varepsilon_\alpha/\varepsilon_\beta$ and the red shift of α and β bands are qualitative correlated with the strength of a coordination bonding of zinc–ligand bond and stability of the complex.[11] Table 1 summarizes the observed α and β bands under various conditions. It is clear that the complexation with pyridine increases $\varepsilon_\alpha/\varepsilon_\beta$, but

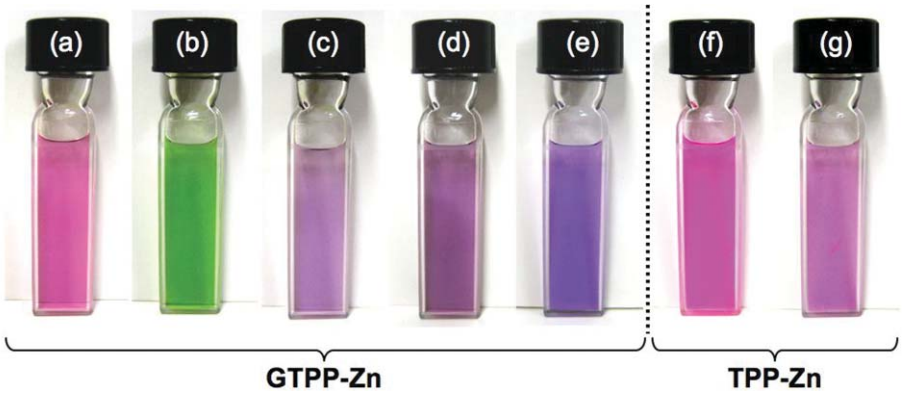

Fig. 2 Library of colour changes of the porphyrin derivatives (0.5 mM) in cyclohexane at 20 °C. (a) **GTPP-Zn**, (b) **GTPP-Zn** with pyridine (10 equiv.), (c) **GTPP-Zn** with pyridine (2000 equiv.), (d) **GTPP-Zn** in chloroform, (e) **GTPP-Zn** with pyridine (10 equiv.) in chloroform, (f) **TPP-Zn**, and (g) **TPP-Zn** with pyridine (10 equiv.).

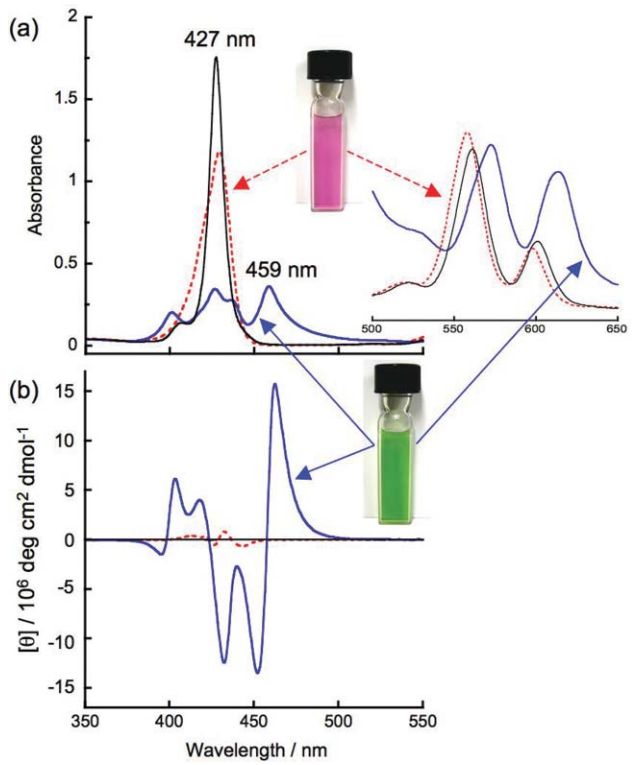

Fig. 3 UV-visible (a) and CD (b) spectra of **GTPP-Zn** (0.25 mM) in cyclohexane at 20 °C without pyridine (red broken line), with 10 equiv. (blue line) and 2000 equiv. (black line) of pyridine.

the most remarkable λ_{max} shifts and enhancement of the $\varepsilon_\alpha/\varepsilon_\beta$ value were observed in the **GTPP-Zn**–pyridine complex. These results indicate that the molecular stacking results in a remarkable increase of the stability of the complex.

For ^{1}H NMR spectroscopy, a sample of the **GTPP-Zn**–pyridine complex was obtained by recrystallization from a concentrated cyclohexane solution and successive washing with cyclohexane. Analysis was performed in a chloroform-*d* solution. The resultant ^{1}H NMR spectrum shows large upfield shifts of the proton resonances of the pyridyl ring ($\Delta\delta^{o\text{-}H}$ = 5.24 ppm, $\Delta\delta^{m\text{-}H}$ = 1.48 ppm) caused by the shielding effect of the porphyrin.[12] This result supports that the complexation of **GTPP-Zn** with

Table 1 Absorption spectral date of **TPP-Zn** and **GTPP-Zn**

Porphyrin[a]	Guest molecule (equiv.)	Solvent	β/nm	α/nm	$\varepsilon_\alpha/\varepsilon_\beta$
TPP-Zn	None	$CHCl_3$	551	594	0.16
	Pyridine (10)	$CHCl_3$	562	602	0.44
	None	Cyclohexane	545	585	0.09
	Pyridine (10)	Cyclohexane	560	599	0.34
	None[b]	Toluene	549	588	0.16
	Pyridine (1)[b]	Toluene	562	602	0.43
GTPP-Zn	None	$CHCl_3$	554	597	0.27
	Pyridine (10)	$CHCl_3$	562	603	0.46
	None	Cyclohexane	558	598	0.33
	Pyridine (10)	Cyclohexane	573	613	0.89
	Pyridine (2000)	Cyclohexane	561	601	0.41

[a] Concentration of porphyrin: 0.25 mM [b] Date from reference 11.

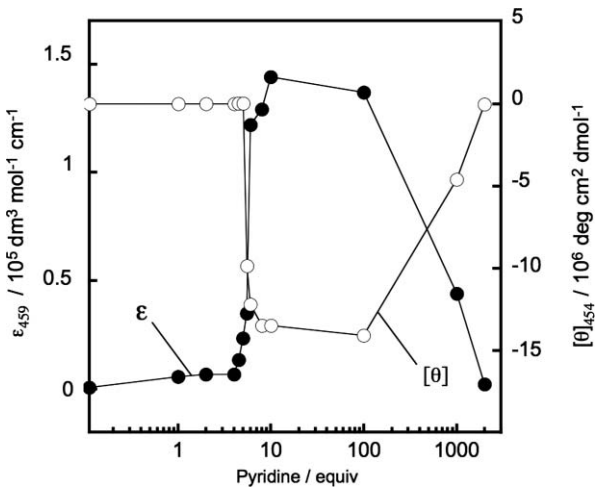

Fig. 4 Concentration dependency of molecular coefficient (ε) at 459 nm and molecular ellipticity ([θ]] at 454 nm of **GTPP-Zn** (0.25 mM) with pyridine (0 to 2000 equiv.) complex at 20 °C.

pyridine is formed by axial coordination. In addition, the binding ratio of **GTPP-Zn** and pyridine was also estimated by the peak areas of a chiral carbon in an L-glutamide moiety and *m*-H in a coordinated pyridine, indicating a one-to-one complex of **GTPP-Zn** and pyridine.†

The IR spectra showed informative absorption shifts on the amide bond.† The typical absorptions of **GTPP-Zn** with pyridine in cyclohexane were located at 1632 cm^{-1} and 1550 cm^{-1} and were attributed to amides I and II, respectively, while nonbonding amide I and II bands measured in a chloroform solution were found at 1652 cm^{-1} and 1525 cm^{-1}, respectively. These results indicate that a strong and ordered hydrogen bonding interaction derived from an L-glutamide moiety is present for the aggregation of **GTPP-Zn**.[13]

A chirally stacked structure of the aggregates can be estimated from a CD spectral pattern. The greenish complex showed a typical splitting with a positive Cotton effect around 462 nm and a negative Cotton effect around 454 nm (Fig. 3b). According to Huang's definition,[6] this pattern can be assigned to a typical *R*-chiral plane-to-plane ordering.

Induction of morphological change

As shown in Fig. 5a, only globular-like structures having diameters of 300–500 nm were observed in the cast film prepared from a cyclohexane solution containing 0.25 mM **GTPP-Zn**. It should be noted that no staining reagent such as heavy metals was used in the sample preparation, and therefore the good contrast of the TEM image supports the existence of zinc ions in the aggregates. This explains that the good solubility of **GTPP-Zn** in nonpolar solvents is due to globular aggregation although free-base **GTPP** forms nanofibrillar aggregates to make a gel.[5]

Fig. 5b shows that the complexation with pyridine induces a drastic change of aggregation morphology from globular to needle-like structures. The dimensions of the newly detected morphology are a minimum diameter of several nanometres and a length of a couple of micrometres. This supports the spectral estimation that the greenish aggregates of a one-to-one complex of **GTPP-Zn** with pyridine would be based on nanocrystals. On the other hand, no similar aggregation was observed in the **TPP-Zn**–pyridine complex. Therefore, the L-glutamide moiety provides as essential driving force for aggregation and ordering on the basis of intermolecular hydrogen bonding interaction.

Selective chiroptical response on axial coordination

UV-visible and CD spectral responses of **GTPP-Zn** (0.25 mM) were investigated for various pyridine derivatives such as monoalkyl- and dialkylpyridines. As shown in Fig. 6, the obtained UV-visible and CD spectra were distinctly different from each other because of the chemical difference of pyridines such as (a) 4-methylpyridine, (b) 3,5-dimethylpyridine, (c) 4-*tert*-butylpyridine, and (d) 2,6-di-*tert*-butylpyridine, as typical examples. For example, strong CD signals were induced by 4-methylpyridine, but the chiral sense at around 450 nm was opposite that in pyridine. On the other hand, 2,6-di-*tert*-butylpyridine induced few CD signals. It is clear that the spectral patterns vary in λ_{max}, sharpness, intensity, chiral sense, and splitting pattern. In addition, the spectral response was accompanied by a change of aggregation morphology. Typical examples are shown in Fig. 7. Both 2,3- and 3,5-dimethylpyridine induced nanofibrillar aggregation (Fig. 7b and 7c), but 2,6-dimethylpyridine did not induce fibrillar structure but rather globular-like structure (Fig. 7d). As compared with Fig. 5b, these morphological changes are clearly different from that in pyridine

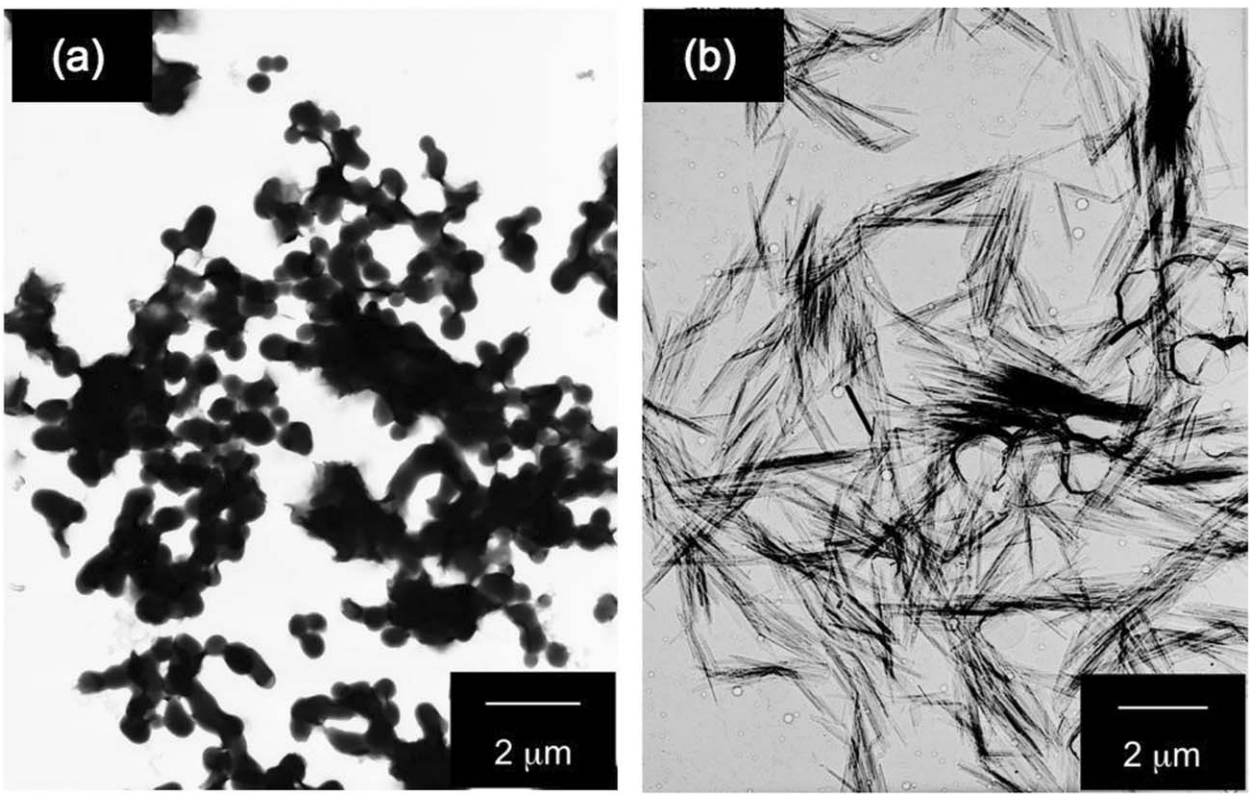

Fig. 5 TEM images of **GTPP-Zn** (a) without and (b) with 10 equiv. of pyridine. The samples were prepared by casting from a 0.25 mM cyclohexane solution and no staining regent was used.

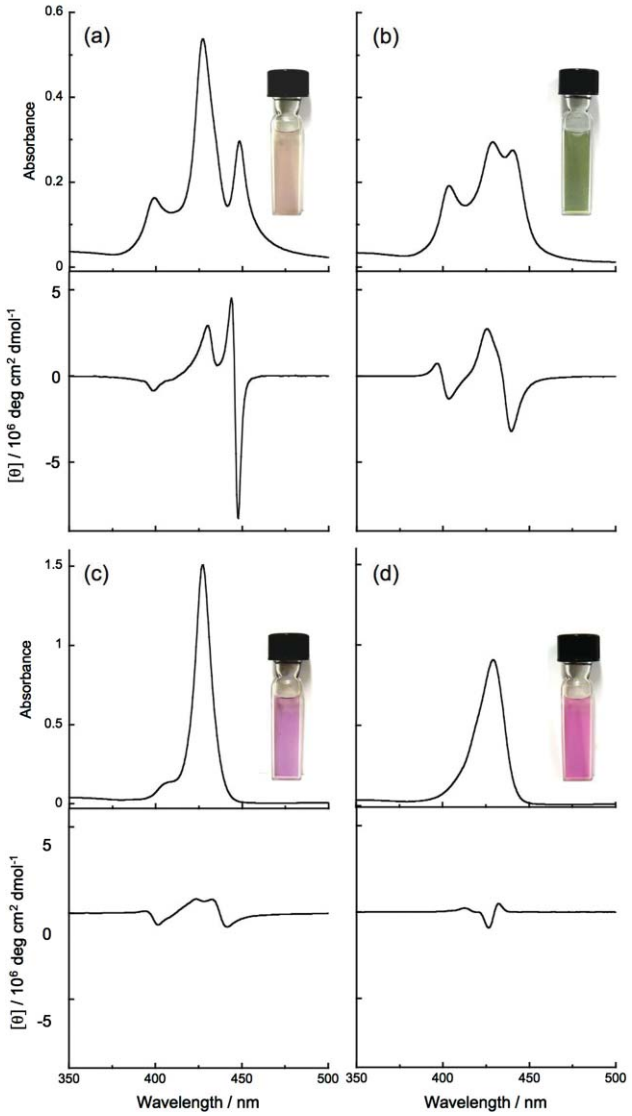

Fig. 6 UV-visible and CD spectra of **GTPP-Zn** (0.25 mM) with 10 equiv. of (a) 4-methylpyridine, (b) 3,5-dimethylpyridine, (c) 4-*tert*-butylpyridine, and (d) 2,6-di-*tert*-butylpyridine in cyclohexane at 20 °C.

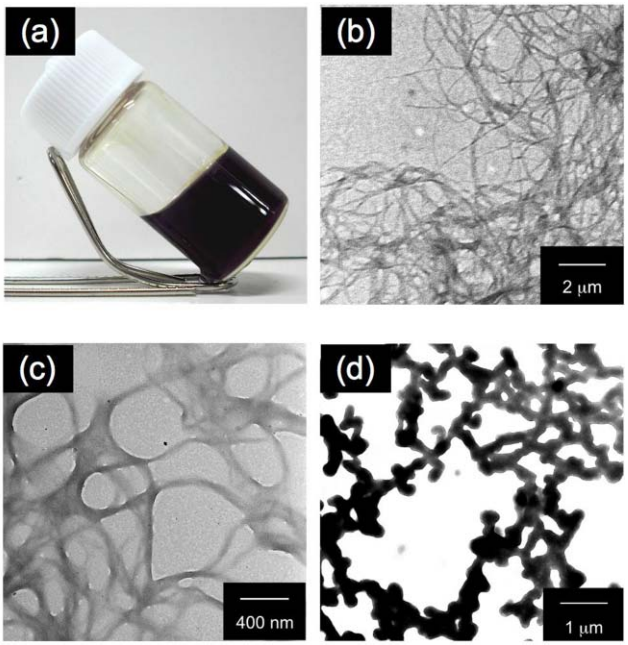

Fig. 7 (a) Photo image of the **GTPP-Zn** (1 mM) gel in cyclohexane at 15 °C with 2,3-dimethylpyridine (100 equiv.). TEM images of the **GTPP-Zn** aggregates with (b) 2,3-dimethylpyridine (100 equiv.), (c) 3,5-dimethylpyridine (10 equiv.), and (d) 2,6-dimethylpyridine (10 equiv.) in the cast film prepared by 0.25 mM cyclohexane solution. (b) and (c) were stained by 2.0 wt% ammonium molybdate.

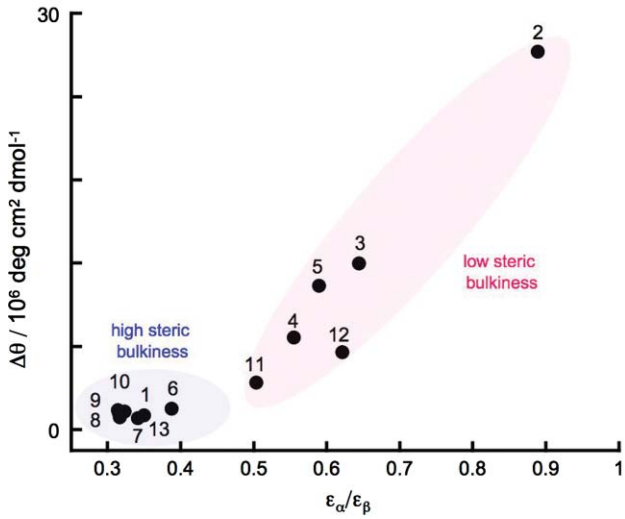

Fig. 8 Plot of $\varepsilon_\alpha/\varepsilon_\beta$ *versus* $\Delta\theta$ values of **GTPP-Zn** (0.25 mM) with 10 equiv. of various guest molecules in cyclohexane at 20 °C. Numbers refer to complexes in Table 2.

where needle-like aggregates were produced. As supporting this, the complexes with 2,3- and 3,5-dimethylpyridine showed a typical mass gelation behavior in 1 mM (Fig. 7a), although the complexation with pyridine promotes the crystallization. These results indicate that the coordination structures influence to the macroscopic morphologies.

These results demonstrate the potential for applicability as a sensing system through axial coordination. In this regard, further detailed investigation was carried out by using 11 kinds of pyridine derivatives as guest molecules. As summarized in Table 2, the λ_{max} shifts of the α and β bands, $\varepsilon_\alpha/\varepsilon_\beta$, and the CD intensity were apparently dependent on the guest molecules. Here, when the focus is on the value of $\varepsilon_\alpha/\varepsilon_\beta$ and the relative CD intensity (Fig. 8), we recognize that there are roughly two classifications in the response pattern: one is to show the results with a weak CD strength as well as a small $\varepsilon_\alpha/\varepsilon_\beta$.

These guest molecules are 2-alkyl and/or *tert*-butyl derivatives. This strongly indicates that **GTPP-Zn** is very sensitive to the steric bulk of the guest molecules. The other one is a category showing the increase of the CD intensity with the increase of the $\varepsilon_\alpha/\varepsilon_\beta$ value although there is one exception in 3,5-dimethylpyridine. However, this exception is probably related to the steric factor derived from two methyl groups. The value of $\varepsilon_\alpha/\varepsilon_\beta$ is an indicator of the complex stability, and therefore it is reasonable that the increase of $\varepsilon_\alpha/\varepsilon_\beta$ is accompanied by an enhancement of chiral ordering, showing an increase of CD strength.

Table 2 Observed α and β bands and the CD intensities of **GTPP-Zn** with various guest molecules in cyclohexane at 20 °C

No.	Guest molecule	β/nm	α/nm	$\varepsilon_\alpha/\varepsilon_\beta$	$[\theta]_{max}$ (10^6 deg cm^2 dmol^{-1})	$[\theta]_{min}$	$\Delta\theta$ ($[\theta]_{max}$ - $[\theta]_{min}$) /10^6 deg cm^2 dmol^{-1}
1	None	558	598	0.33	433 (0.8)	443 (0.7)	1.5
2	Pyridine	573	613	0.89	462 (15.9)	454 (13.2)	29.1
3	4-Methylpyridine	566	603	0.64	444 (4.5)	448 (8.3)	12.8
4	3-Methylpyridine	564	603	0.56	426 (3.3)	439 (3.8)	7.1
5	3-Ethylpyridine	565	604	0.59	426 (6.2)	440 (4.9)	11.1
6	4-*tert*-Butylpyridine	561	602	0.39	424 (0.8)	442 (0.8)	1.6
7	2,3-Dimethylpyridine	559	598	0.34	432 (0.4)	426 (0.5)	0.9
8	2,4-Dimethylpyridine	558	598	0.32	432 (0.4)	426 (0.5)	0.9
9	2,5-Dimethylpyridine	558	598	0.32	432 (0.5)	426 (0.8)	1.3
10	2,6-Dimethylpyridine	558	598	0.32	432 (0.5)	420 (0.9)	1.4
11	3,4-Dimethylpyridine	565	602	0.50	425 (2.4)	399 (1.3)	3.7
12	3,5-Dimethylpyridine	565	604	0.62	426 (2.7)	440 (3.2)	15.9
13	2,6-Di-*tert*-butylpyridine	559	599	0.35	434 (0.6)	427 (0.5)	1.1

Concentration of **GTPP-Zn**: 0.25 mM, guest molecule: 2.5 mM (10 equiv.).

Conclusions

In this paper, we have described the synthesis of a new zinc-inserted porphyrin lipid (**GTPP-Zn**) and the chiroptical response toward pyridine derivatives. The following findings can be summarized: (1) the solubility in a nonpolar solvent was fully modified by insertion of zinc into **GTPP** compared with free-base **GTPP**. TEM observations indicated that the solubility improvement was related to a change in aggregation morphology from fibrils to globules. As a result, **GTPP-Zn** showed lyotropic and thermotropic aggregate-to-monomer transitions in nonpolar organic solvents such as cyclohexane. (2) Axial coordination of pyridine on **GTPP-Zn** induced new chirality in the Soret band as well as a drastic visible spectral change. This is caused by induction of highly ordered chiral stacking among the porphyrin moieties. (3) By investigation of axial coordination with various pyridine derivatives, it was confirmed that the resultant spectral patterns varied in intensity, shift, and splitting. This indicates that **GTPP-Zn** has high potential applicability as a multiresponsive molecular switching device.

Experimental

Materials and instrumentations

5-(4-Methoxycarbonylphenyl)-10,15,20-triphenyl-21*H*,23*H*-porphine and 5,10,15,20-tetraphenyl-21*H*,23*H*-porphine were purchased from the Tokyo Chemical Industry. Reagent grade solvents and Measurement grade solvent were purchased from Nacalai tesque. N^1,N^5-didodecyl-L-glutamide (**G**) was synthesized by the previously reported procedure[5] with slight modification. ^{1}H NMR (400 MHz) spectra were recorded in $CDCl_3$ with $SiMe_4$ as an internal standard with JNM-EX400 (JEOL). FT-IR spectra were measured in a KBr method with FT/IR-4100 (JASCO). FT-IR spectra of solution were obtained from 1 mM cyclohexane or chloroform solutions. MALDI TOF-MS spectrum was recorded on a Voyager RP (PerSeptiv Biosystem). UV-visible and CD spectra were measured with V-560 (JASCO) and J725 (JASCO), respectively. The solution was poured into a 0.1 mm, 1.0 mm and 10 mm quartz cell. TEM images were observed with JEM-2000X (JEOL). The solution was cast in a carbon-coated copper grid and dried by a vacuum pump under reduced pressure. The accelerating voltage of the TEM was 80 kV and the beam current was 40 A.

Zinc inserted porphyrin-lipid (GTPP-Zn)

Zinc inserted porphyrin (**GTPP-Zn**) was prepared by mixing a solution of $Zn(OAc)_2$ $2H_2O$ (0.17 g, 0.80 mmol) in methanol (10 mL) and a solution of **GTPP** (0.3 g, 0.25 mmol), which was obtained by the previously reported procedure[7] in chloroform (100 mL). The mixture solution was stirred for 6 h at room temperature. The solution was concentrated in vacuo. The residue was redissolved in chloroform, and the organic layer was washed with water and dried with sodium sulfate. The solution was dried *in vacuo* to give purple solids (196 mg, 72%). mp: 230.5–232.5 °C. (Found: C, 74.56; H, 7.28; N, 8.21. $C_{74}H_{85}N_7O_3Zn$ requires C, 74.95; H, 7.22; N, 8.27%). ν_{max}(KBr)/cm^{-1} 3395 and 3310 (NH), 2925 and 2852 (CH), 1647 (CO), 1523 (NH). δ_H (400 MHz; $CDCl_3$; Me_4Si) 0.79–0.86 (6H, t, $-CH_3$), 1.16–1.25 (40H, br, $-(CH_2)_{10}-$), 1.54 (2H, br, $-CH_2CO-$), 1.75–1.91 (2H, br, $-CH_2-$), 2.67–2.81 (4H, m, $-NHCH_2-$), 3.46 (1H, q, –CH–), 5.56 (1H, br, NH), 6.28 (1H, br, NH), 7.45–7.51 (1H, br, NH), 7.74–7.76 (9H, m, ArH), 8.13–8.22 (10H, m, ArH), 8.80–8.94 (8H, m, ArH). MALDI TOF MS (2,5–dihydroxybenzoic acid matrix): Calcd for $C_{74}H_{85}N_7O_3Zn$ 1183.60, m/z = 1184.45 (M^+).

Acknowledgements

This work was supported in part by a Grant-in-Aid for Scientific Research from the Ministry of Education, Science, Sports, and Culture of Japan.

Notes and references

1 L. Yuan, R. Wang and D. H. Macartney, *Tetrahedron: Asymmetry*, 2007, **18**, 483–487; D. Monti, L. L. Monica, A. Scipioni and G. Mancini, *New J. Chem.*, 2001, **25**, 780–782; M. Mathews and N. Tamaoki, *J. Am. Chem. Soc.*, 2008, **130**, 11409–11416; A. Shundo, J. Labuta, J. P. Hill, S. Ishihara and K. Ariga, *J. Am. Chem. Soc.*, 2009, **131**, 9494–9495; A. Patel, S. Fouace and J. H. G. Steinke, *Anal. Chim. Acta*, 2004, **504**, 53–62.

2 B. L. Feringa, *Acc. Chem. Res.*, 2001, **34**, 504–513; M. Takafuji, A. Ishiodori, T. Yamada, T. Sakurai and H. Ihara, *Chem. Commun.*, 2004, 1122–1123.

3 Y.-C. Lin and R. G. Weiss, *Macromolecules*, 1987, **20**, 414–417; J. H. Van Esch and B. L. Feringa, *Angew. Chem., Int. Ed.*, 2000, **39**, 2263–2266; N. Ide, T. Fukuda and T. Kunitake, *Bull. Chem. Soc. Jpn.*, 1995, **68**, 3423–3428; T. Shimizu, M. Masuda and H. Minamikawa, *Chem. Rev.*, 2005, **105**, 1401–1443; M. Suzuki, T. Sato, A. Kurose, H. Shirai and K. Hanabusa, *Tetrahedron Lett.*, 2005, **46**, 2741–2745; P. Xue, R. Lu, D. Li, M. Jin, C. Tan, C. Bao, Z. Wang and Y. Zhao, *Langmuir*, 2004, **20**, 11234–11239.

4 J.-H. Fuhrhop, C. Demoulin, C. Boettcher, J. Koning and U. Siggel, *J. Am. Chem. Soc.*, 1992, **114**, 4159–4165; S. Tamaru, M. Nakamura, M. Takeuchi and S. Shinkai, *Org. Lett.*, 2001, **3**, 3631–3634; F. Würthner, Z. Chen, F. J. M. Hoeben, P. Osswald, C.-C. You, P. Jonkheijm, J. V. Herrikhuyzen, A. P. H. J. Schenning, P. P. A. M. van der Schoot, E. W. Meijer, E. H. A. Beckers, S. C. J. Meskers and R. A. J. Janssen, *J. Am. Chem. Soc.*, 2004, **126**, 10611–10618; S. Cicchi, G. Ghini, S. Fallani, A. Brandi, D. Berti, F. Betti and P. Baglioni, *Tetrahedron Lett.*, 2008, **49**, 1701–1705; H. Ihara, T. Sakurai, T. Yamada, T. Hashimoto, M. Takafuji, T. Sagawa and H. Hachisako, *Langmuir*, 2002, **18**, 7120–7123.

5 H. Ihara, M. Yoshitake, M. Takafuji, T. Yamada, T. Sagawa, C. Hirayama and H. Hachisako, *Liq. Cryst.*, 1999, **26**, 1021–1027.

6 X. Huang, B. H. Rickman, B. Borhan, N. Berova and K. Nakanishi, *J. Am. Chem. Soc.*, 1998, **120**, 6185–6186; D. P. Cormode, S. S. Murray, A. R. Cowley and P. D. Beer, *Dalton Trans.*, 2006, 5135–5140; J. P. Hill, Y. Wakayama, W. Schmitt, T. Tsuruoka, T. Nakanishi, M. L. Zandler, A. L. McCarty, F. D'Souza, L. R. Milgrom and K. Ariga, *Chem. Commun.*, 2006, 2320–2322; Y. Li, T. Wang and M. Liu, *Soft Matter*, 2007, **3**, 1312–1317; N. C. Maiti, S. Mazumdar and N. Periasamy, *J. Phys. Chem. B*, 1998, **102**, 1528–1538; M. V. Rekharsky, H. Yamamura, C. Inoue, M. Kawai, I. Osaka, R. Arakawa, K. Shiba, A. Sato, Y. H. Ko, N. Selvapalam, K. Kim and Y. Inoue, *J. Am. Chem. Soc.*, 2006, **128**, 14871–14880.

7 H. Jintoku, T. Sagawa, T. Sawada, M. Takafuji, H. Hachisako and H. Ihara, *Tetrahedron Lett.*, 2008, **49**, 3987–3990.

8 P. Terech, R. G. Weiss, ed. *Chem. Rev.*, 1997, **97**, 3133-3159; R. Oda, *Molecular Gels: Materials with Self-assembled Fibrillar Networks*, R. G. Weiss and P. Terech, ed.; Springer, Berlin, 2006, 577-612; J-P. Desvergne, A. G. L. Olive, N. M. Sangeetha, J. Reichwangen, H. Hopf and A. D. Guerzo, *Pure Appl. Chem.*, 2006, **78**, 2333–2339; G. Clavier, M. Mistry, F. Fages and J-L. Pozzo, *Tetrahedron Lett.*, 1999, **40**, 9021–9024.

9 J.-S. Hu, Y.-G. Guo, H.-P. Liang, L.-J. Wan and L. Jiang, *J. Am. Chem. Soc.*, 2005, **127**, 17090–17095.

10 V. Huber, M. Lysetska and F. Wurthner, *Small*, 2007, **3**, 1007–1014; T. Kishida, N. Fujita, O. Hirata and S. Shinkai, *Org. Biomol. Chem.*, 2006, **4**, 1902–1909; T. S. Balaban, *Acc. Chem. Res.*, 2005, **38**, 612–623.

11 M. Nappa and J. S. Valentine, *J. Am. Chem. Soc.*, 1978, **100**, 5075–5080; G. Szintay and A. Horváth, *Inorg. Chim. Acta*, 2000, **310**, 175–182.

12 V. F. Slagt, P. C. J. Kamer, P. W. N. M. van Leeuwen and J. N. H. Reek, *J. Am. Chem. Soc.*, 2004, **126**, 1526–1536; P. N. Taylor and H. L. Anderson, *J. Am. Chem. Soc.*, 1999, **121**, 11538–11545.

13 N. Yamada, K. Ariga, M. Naito, K. Matsubara and E. Koyama, *J. Am. Chem. Soc.*, 1998, **120**, 12192–12199; M. Suzuki, C. Setoguchi, H. Shirai and K. Hanabusa, *Chem.–Eur. J.*, 2007, **13**, 8193–8200.

